Supporting Information for

# Synergistic Effect of Cation and Anion for Low-Temperature Aqueous Zinc-Ion Battery

Tianjiang Sun[1], Shibing Zheng[1], Haihui Du[1], Zhanliang Tao[1,*]

[1]Key Laboratory of Advanced Energy Materials Chemistry (Ministry of Education), Renewable Energy Conversion and Storage Center, College of Chemistry, Nankai University, Tianjin 300071, P. R. China

*Corresponding author. E-mail: taozhl@nankai.edu.cn (Zhanliang Tao)

## Supplementary Figures and Table

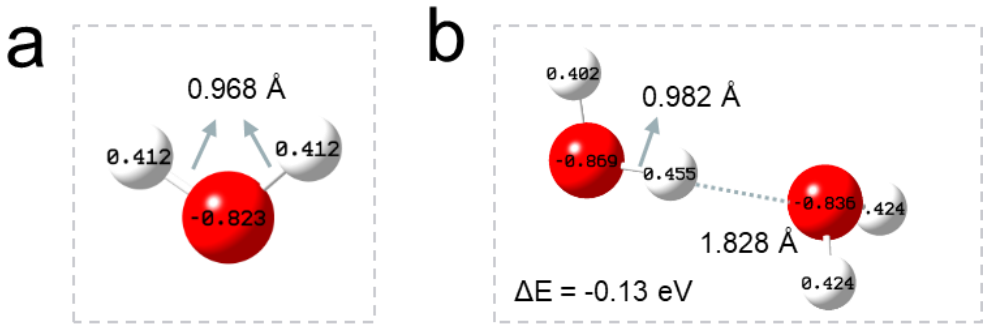


**Fig. S1 a**) Optimal structure of water molecule. **b**) The combining energy of two molecules and corresponding structure information

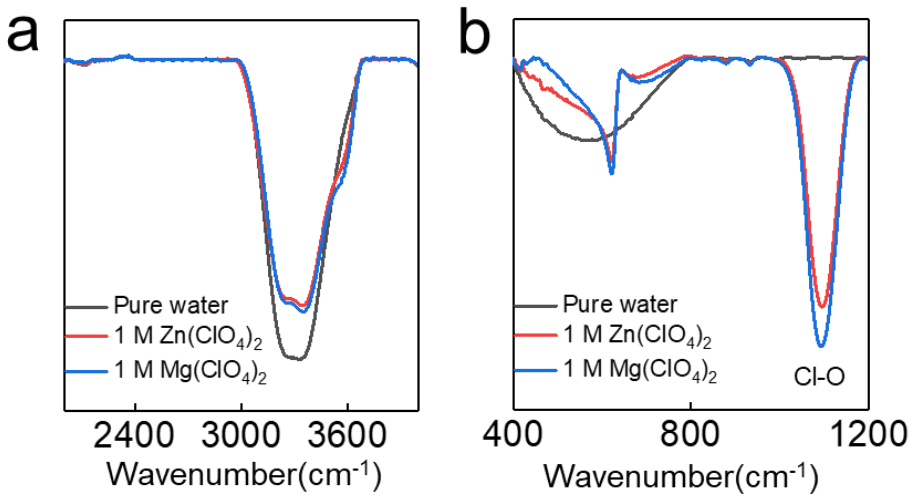


**Fig. S2 a**) FTIR spectra of O-H bond. **b**) FTIR spectra of Cl-O

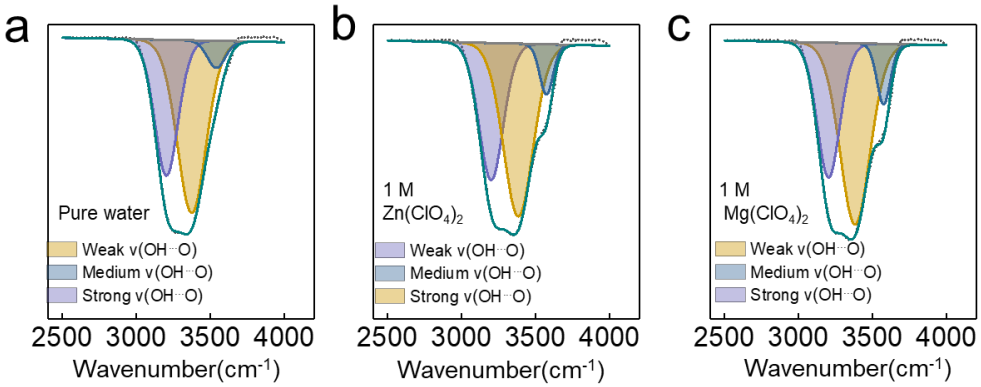


**Fig. S3** The fitted O–H stretching vibration representing water molecules with strong, medium and weak HBs. **a**) Pure water. **b**) 1 M $Zn(ClO_4)_2$. **c**) 1 M $Mg(ClO_4)_2$

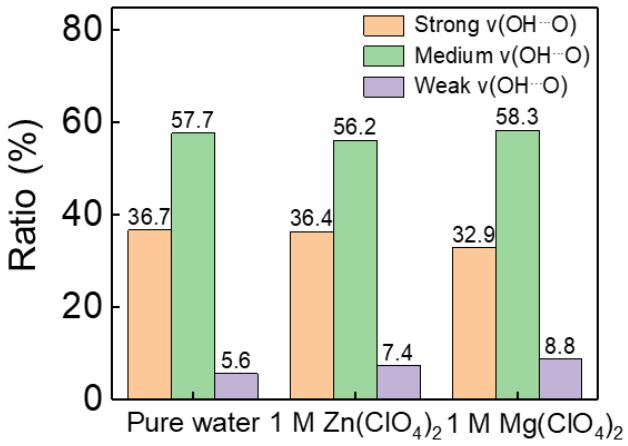


**Fig. S4** The ratio of different types of HBs

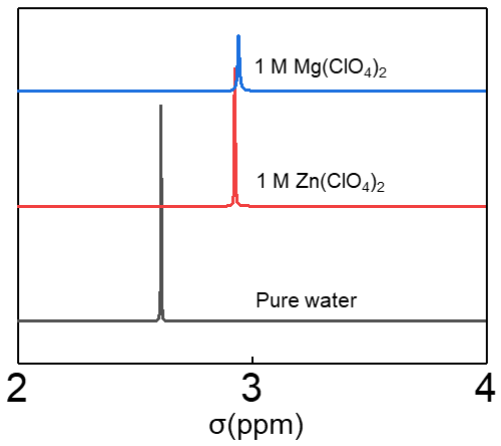


**Fig. S5** $^1H$ NMR spectra of different solutions

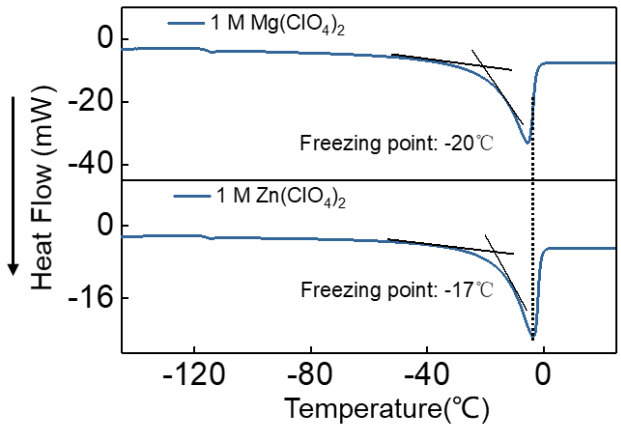


**Fig. S6** The freezing points of different solutions

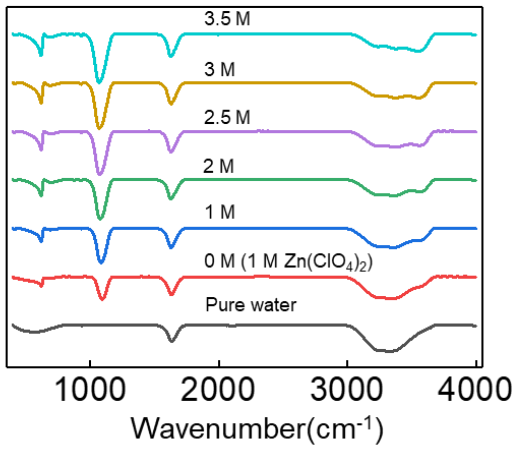


**Fig. S7** The all FT-IR spectra of different concentration electrolytes

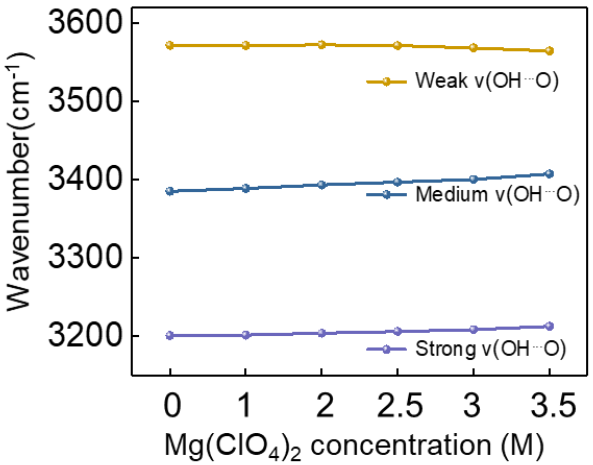


**Fig. S8** The wavenumber shift of different types of HBs

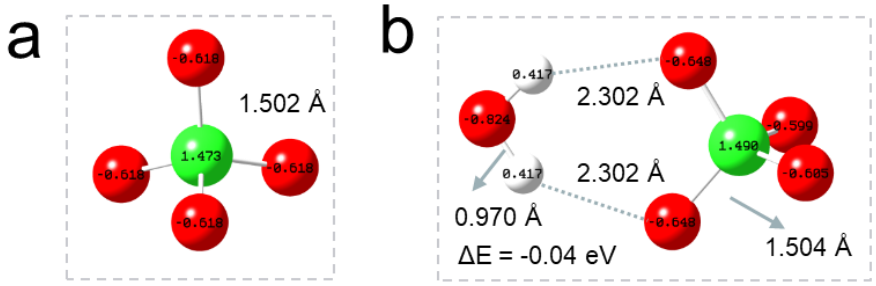


**Fig. S9 a**) Optimal structure of $ClO_4^-$. **b**) Combining energy between $ClO_4^-$ and $H_2O$ and corresponding structure information

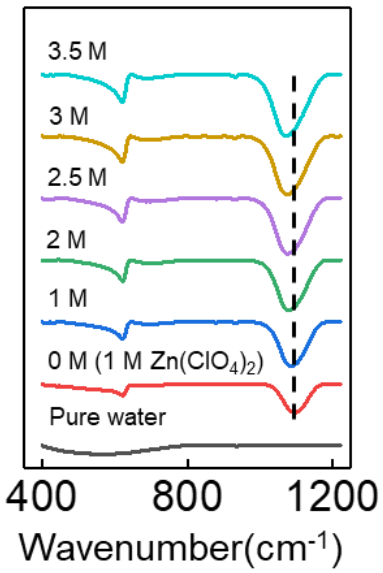


**Fig. S10** FTIR spectra of Cl-O bond

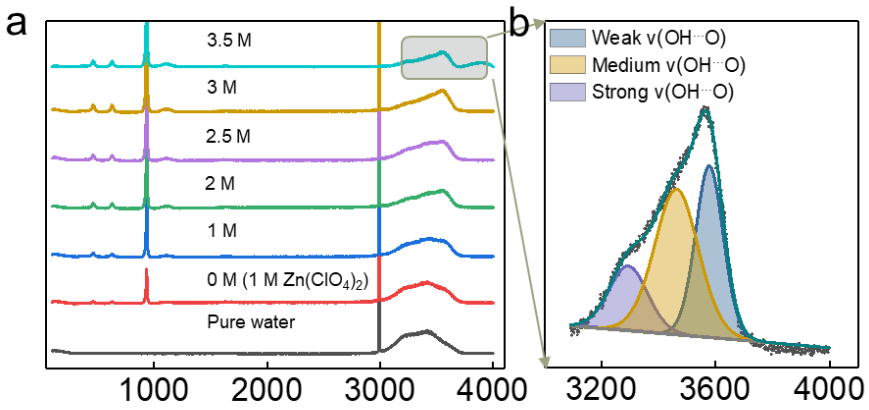


**Fig. S11 a**) All Raman spectra of different concentration electrolytes. **b**) The fitted O–H stretching vibration representing water molecules with strong, medium and weak HBs

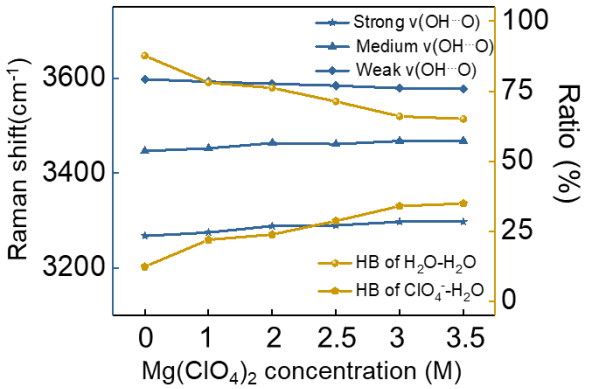


**Fig. S12** The ratio and Raman shift of different types of HBs

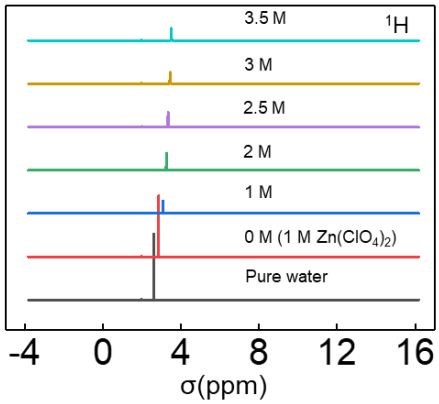


**Fig. S13** The all $^{1}$H NMR spectra of different concentration electrolytes

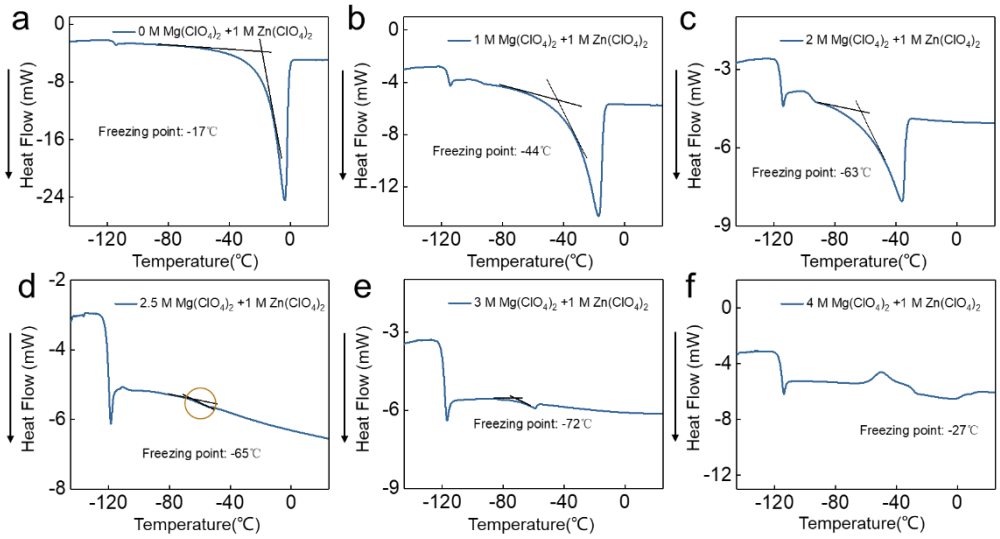


**Fig. S14** DSC curves of **a**) 0 M (1 M $Zn(ClO_4)_2$); **b**) 1 M; **c**) 2 M; **d**) 2.5 M; **e**) 3 M; **f**) 4 M solution

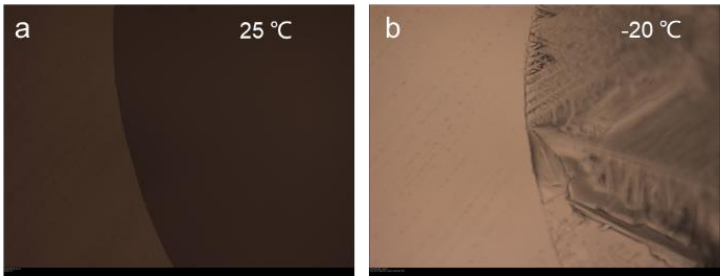


**Fig. S15** The non-polarizing light microscope observation of 0 M electrolyte (1 M $Zn(ClO_4)_2$) at **a**) 25 °C; **b**) -20 °C

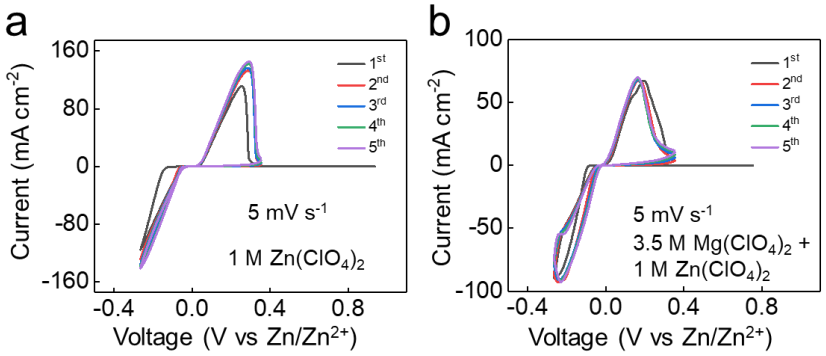


**Fig. S16** CV curves of Zn||SS at **a**) 1 M $Zn(ClO_4)_2$; **b**) 3.5 M $Mg(ClO_4)_2$ + 1 M $Zn(ClO_4)_2$ electrolyte

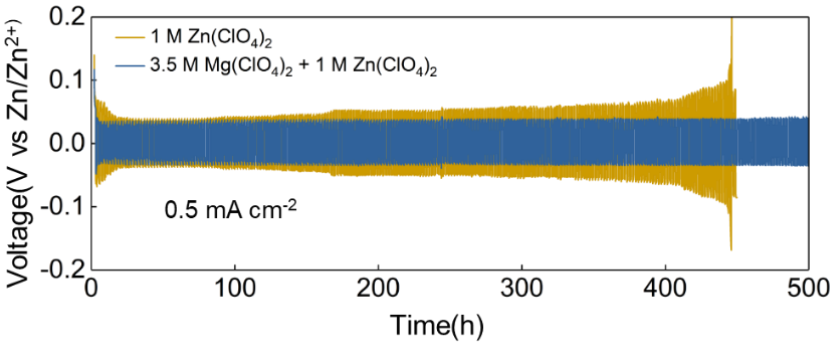


**Fig. S17** The cycling stability of Zn||Zn battery at different electrolytes

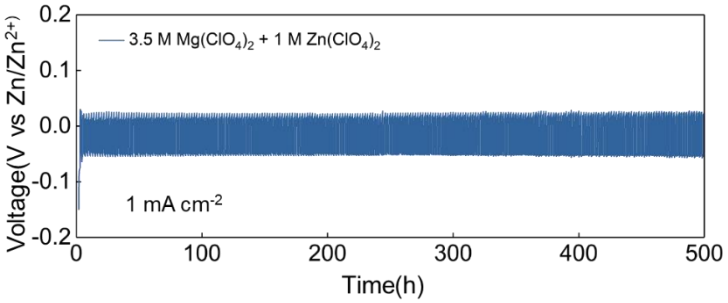


**Fig. S18** The cycling stability of Zn||Zn battery at 3.5 M electrolyte

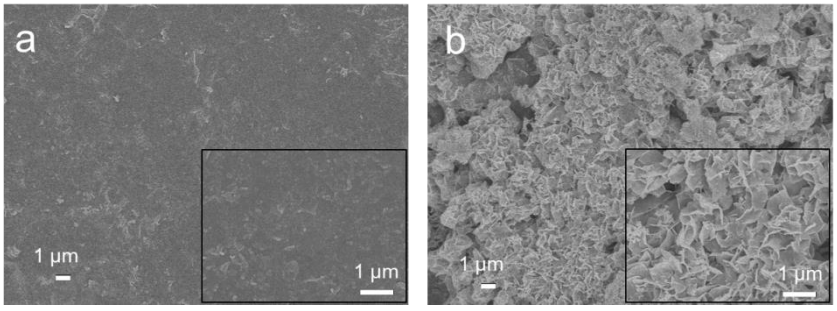


**Fig. S19** SEM images of Zn **a**) at 3.5 M electrolyte; **b**) at 1 M $Zn(ClO_4)_2$ electrolyte

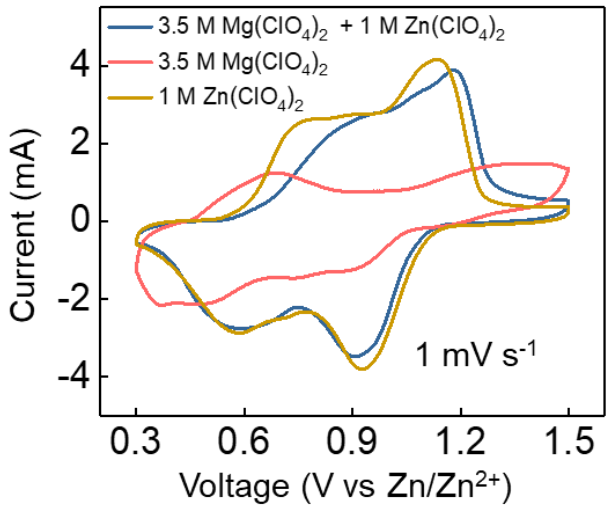


**Fig. S20** CV curves of Zn||PTO battery at different electrolytes

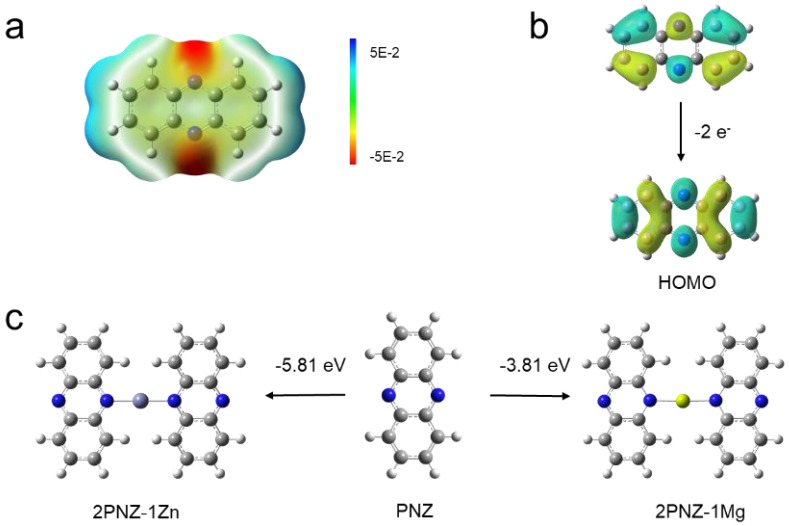


**Fig. S21 a**) ESP of PNZ. **b**) HOMO plots of PNZ and $PNZ^{2-}$. **c**) The corrected binding energies of PNZ with $Zn^{2+}$ or $Mg^{2+}$

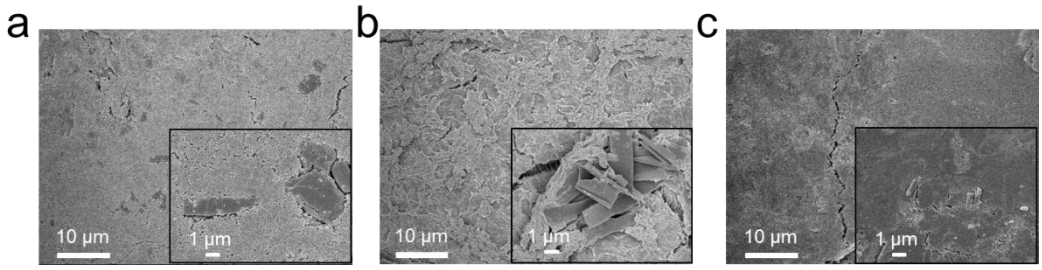


**Fig. S22** SEM images of PTO electrodes at **a**) Initial state; **b**) Discharge state; **c**) Charge state

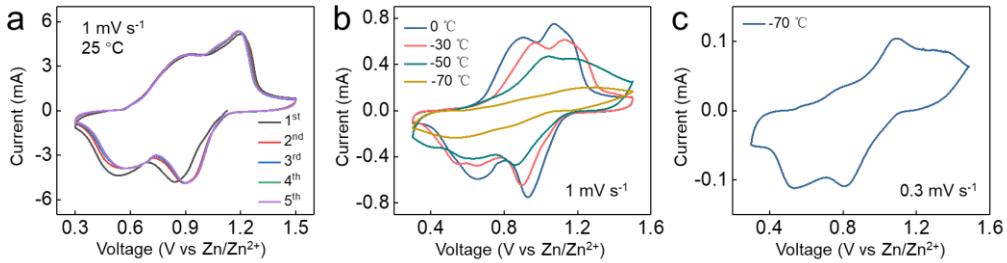


**Fig. S23** CV curves of Zn||PTO battery at **a**) 25 °C; **b**) 0, -30 °C, -50 °C and -70 °C; **c**) -70 °C and 0.3 mV $s^{-1}$

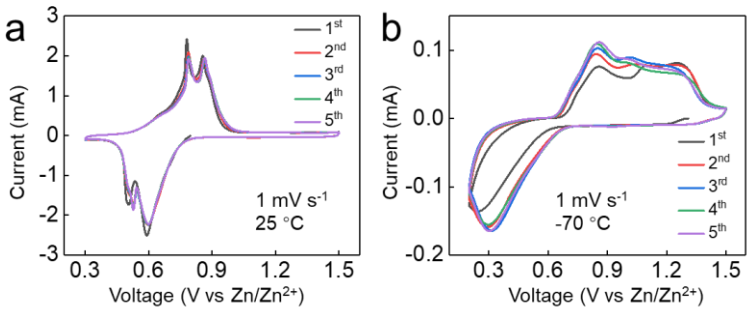


**Fig. S24** CV curves of Zn||PNZ battery at **a**) 25 °C; **b**) -70 °C

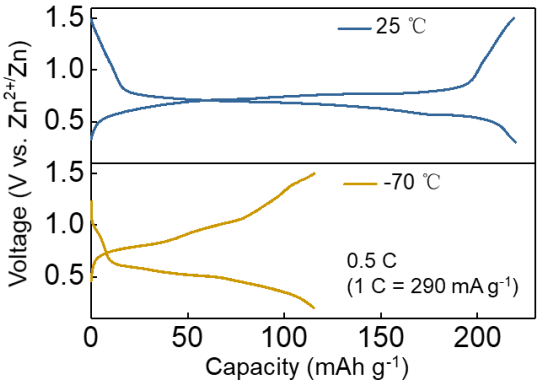


**Fig. S25** The charge-discharge curves of Zn||PNZ battery at 25 °C and -70 °C

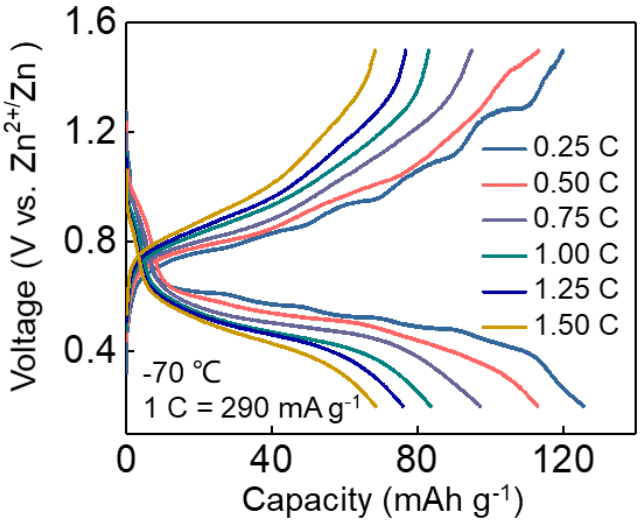


**Fig. S26** The rate capacity of Zn||PNZ battery at -70 °C

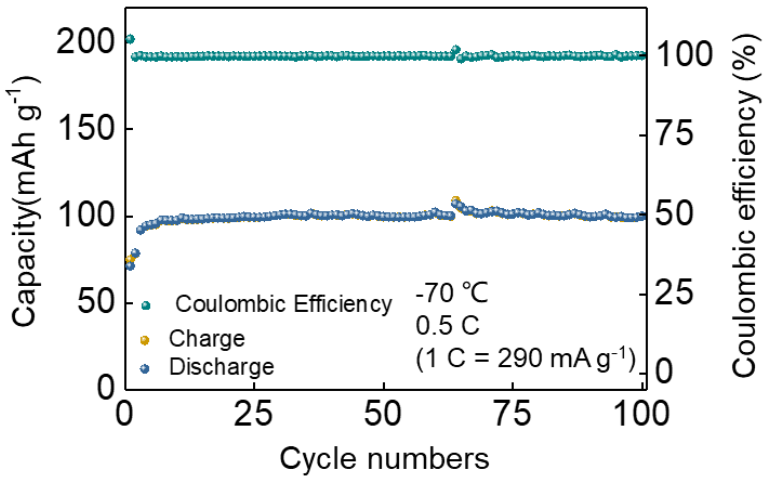


**Fig. S27** The cycling stability of Zn||PNZ battery at -70 °C

**Table S1** DES of PTO electrodes at different states

| | C (atom%) | O (atom%) | Zn (atom%) | Mg (atom%) |
|---|---|---|---|---|
| Initial | 87.26 | 12.74 | 0 | 0 |
| Discharge | 53.42 | 34.47 | 11.90 | 0.22 |
| Charge | 84.41 | 10.67 | 4.92 | 0 |